Radiation Protection Dosimetry (2015), pp. 1–5 doi:10.1093/rpd/ncv292

ENERGY DEPENDENCE OF THE COMPLEXITY OF DNA DAMAGE INDUCED BY CARBON IONS

D. Alloni[1,2,3,*], G. Baiocco[1,3], G. Babini[1,3], W. Friedland[4], P. Kundrát[4], L. Mariotti[1,3,5] and A. Ottolenghi[1,3]
[1]Department of Physics, University of Pavia, Via Bassi 6, Pavia, Italy
[2]LENA, Laboratory of Applied Nuclear Energy, University of Pavia, Via Aselli 41, Pavia, Italy
[3]INFN National Institute of Nuclear Physics, Sezione di Pavia, Via Bassi 6, Pavia, Italy
[4]Institute of Radiation Protection, Helmholtz Zentrum München, Neuherberg 85764, Germany
[5]Department of Oncology, Gray Institute for Radiation Oncology and Biology, Old Road Campus Research Building, Off Roosevelt Drive, Oxford OX3 7DQ, UK

*Corresponding author: daniele.alloni@unipv.it

To assess the complexity of DNA damage induced by carbon ions as a function of their energy and LET, 2-Gy irradiations by 100 keV u^{-1}–400 MeV u^{-1} carbon ions were investigated using the PARTRAC code. The total number of fragments and the yield of fragments of <30 bp were calculated. The authors found a particularly important contribution of DNA fragmentation in the range of <1 kbp for specific energies of <6 MeV u^{-1}. They also considered the effect of different specific energies with the same LET, i.e. before and after the Bragg peak. As a first step towards a full characterisation of secondary particle production from carbon ions interacting with tissue, a comparison between DNA-damage induction by primary carbon ions and alpha particles resulting from carbon break-up is presented, for specific energies of >1 MeV u^{-1}.

INTRODUCTION

Energy deposition by ionising radiation produces critical cellular lesions such as DNA double-strand breaks (DSBs), which may later lead to the manifestation of relevant biological endpoints[1]. The probability of a given late cellular effect does not depend only on the number of DSBs produced but also on their spatial distribution[2]. In particular, if two or several DNA lesions are close, they are likely repaired with less efficiency with respect to isolated molecular damage[3]. The sites of these damages may be geometrically close even if their genomic distance (measured in terms of base pairs) is large, due to the chromatin structure conformation. The DSB distribution is also determined by the radiation track structure at the nanometre level, corresponding to the DNA double-helix diameter[4, 5]. Therefore, it is not surprising that the cellular effects induced by a given dose will depend on the radiation quality[6]. It is also well known that at low doses, different radiation qualities are able to induce damage in cells close to the irradiated ones, but not being irradiated themselves. Also in this case, the severity of the damage depends upon radiation qualities to which 'directly-hit' cells were exposed[7, 8]. However, this work is limited to the biological effects related to the complexity of DNA damage in directly exposed cells, which affects their DNA repair mechanisms.

These effects can be evaluated by track structure calculations[9, 10] coupled to a realistic description of the human genome and of the physico-chemical processes leading to DNA damage.

In particular, the focus of this work is on carbon ions, due to the obvious therapeutic interest. Concerning the evaluation of biological damage induction in carbon therapy, one need to consider that carbon interactions with tissue may result in the production of different secondary charged particle species, hence modifying radiation quality and dose delivery along the track[11–13]. This is notably at the basis of the appearance of the fragmentation tail beyond the Bragg peak. Therefore, besides the primary carbon ion effects in terms of DNA damage, one must also take into account damage induction by secondary hadrons produced by nuclear reactions. In general, light particles are mainly produced in inelastic nuclear interactions of primary ions with the target. In the case of carbon, in particular, H- and He-isotopes are most likely to be produced, these latter being formed predominantly in the break-up of ^{12}C into three alphas[13]. Alpha fragments are very stable nuclei with respect to other light ones because of their high binding energy per nucleon (≈7 MeV), and this aspect gives rise to nuclear clustering phenomena, so that an excited carbon nucleus can be populated in an alpha-clustered state and consequently break up into its three alpha constituents even with a small amount of available energy (separation energy $S_{3\alpha} = 7.27$ MeV). Production of alpha particles from projectile fragmentation has to be taken into account especially when passive energy beam degraders are used in carbon ion treatment, as in the case of a fixed-energy beam machine. This implies that a precise and detailed determination of DSB distributions from primary ion is

only the first step in the construction of the relationship between track structure and late cellular effects.

In this work, carbon-induced DNA damage is investigated with the PARTRAC code in a wide range of energy and LET. Results on DNA fragmentation are given in terms of DSB and cluster lesion (CL) (resulting in fragments of <30 bp) induction. As a first step towards a full characterisation of secondary particle production from carbon ions interacting with tissue, the authors also propose a feasibility study on the comparison between DNA fragmentation induced by carbon ions and by secondary alpha particles, for specific energies of >1 MeV u^{-1}.

MATERIALS AND METHODS

Monte Carlo simulations were performed using the PARTRAC code, which includes an accurate representation of the chromatin and of the physical and physicochemical processes associated with energy deposition by radiation. In particular, the target is the whole genome of a human cell in its interphase and it is structured in six levels of DNA organisation (deoxynucleotide pair, double helix, nucleosome, chromatin fibre, chromatin fibre loops and chromosome territories). In this work, the target cell is modelled with two concentric cylinders, the inner one with base radius of 7.5 μm and height of 5 μm (nuclear compartment), and the outer one with base radius of 12.5 μm and height of 15 μm (cell cytoplasmic plus nuclear compartment). For the density of both cell and nucleus, a value of 1.06 g cm^{-3} was chosen. Different modules of the code simulate the various stages after the passage of an ionising particle. Further details on PARTRAC can be found elsewhere[10].

In particular, the transport of ions in the physical module of the PARTRAC code is based on cross sections for the interactions of protons in water[10], which have been suitably extended to reproduce the physics of any type of primary ion in the non-relativistic regime using scaling laws related to the mean free path of the primary ion and to the ion effective charge[14] (Barkas formula). Through the introduction of an effective charge, charge pickup and stripping processes in the low-energy regime can be partially taken into account. For such low energies, an improved cross section data set for the PARTRAC code is currently under development[15]. Published results on DNA fragmentation, obtained from simulations with different ions of interest for basic radiobiology, hadrontherapy and space radiation protection, provided in the past a successful validation of the code for heavy ions[16, 17].

RESULTS

Carbon ions induced damage

DNA damage induced by carbon ions with specific energies ranging from 100 keV u^{-1} up to 400 MeV u^{-1} (see the legend in Figure 1) and for a total dose of 2 Gy was investigated, focusing on the dependence on energy and LET.

The authors have also considered the effect of different specific energies with the same LET, i.e. before and after the Bragg peak.

In this work, each PARTRAC simulation for a total dose of 2 Gy was run ten times, in order to have significant statistics for damage scoring. DNA-damage outcome, shown in Figure 1, was considered in terms of the number of DNA fragments in the ranges: 0–30, 30–1000, 1000–9000, 9000–23 100, 23 100–10^6 and 10^6–5.7×10^6 base pairs (bp). The total number of DSBs is scored together with that of CLs (<30 bp), assumed to be very important for late cellular consequences.

The nominal specific energy was calculated at the centre of the cell nucleus, thus taking into account energy losses both in the Mylar build-up layer (necessary to achieve the electronic equilibrium) and at the entrance of the cell (see Table 1).

The authors found a particularly important contribution of DNA fragmentation in the range of <1 kbp for carbon-specific energies of <6 MeV u^{-1}. The total number of fragments and the yield of fragments of <30 bp were also calculated as a function of specific energy (see Figure 2) and LET (see Figure 3).

In particular, in Figure 4, the fragment yield at the same LET but at the opposite sides of Bragg peak is indicated by dashed circles.

Alpha-induced DNA damage

Three alphas may be produced from carbon break-up, provided enough energy is available in the centre-of-mass of the reaction (e.g. $\sim$1 MeV u^{-1} for C + O interactions), and explore a wide range of energies in their slowing down.

The authors started calculating the total number of fragments and the yield of fragments of <30 bp for chosen specific energies of >1 MeV u^{-1} (see Table 1). As for the carbon-induced damage, PARTRAC was run ten times for a total dose of 2 Gy, but a per-track normalisation (to the number of tracks passing through the nucleus) is now adopted to compare the results for the total number of DSBs and CLs for carbon ions and alpha particles (Figure 4).

Provided that enough energy is available and that the kinematic boost of the reaction is high enough to direct the alphas onto the same cell layer, three alpha tracks replace a decaying carbon track, with roughly the same specific energy. Therefore, a factor of 3 may be applied to directly compare carbon- and alpha-induced DNA damage, as reported in Figure 5. Limited to this feasibility study, this assumption is coherent with the finding of a dominance of secondary alphas in a narrow cone around the carbon beam axis in case of fragmentation in a water phantom[13].

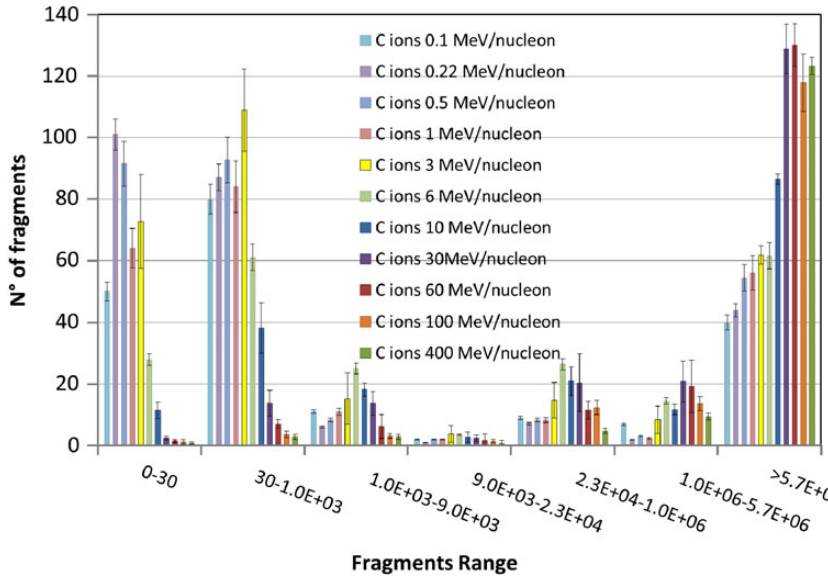

Figure 1. Number of fragments in various length ranges for 2-Gy irradiations with the indicated carbon-specific energies. Error bars correspond to standard deviations ($\pm 1\sigma$).

Table 1. Carbon ion and alpha-specific energies calculated at the centre of the cell nucleus (first column), initial specific energy (second column), mylar thickness and LET (third and fourth columns, respectively).

E_{spec} @ centre (MeV u^{-1})	E_{spec} init (MeV u^{-1}) carbon (alpha)	Mylar (μm) carbon (alpha)	LET (keV μm^{-1}) carbon (alpha)
0.1	0.183	0.1 (0.3)	650
0.22	0.460	0.1	930
0.5	0.750	0.3	930.9
1	1.160 (1.08)	0.3 (0.3)	746.6 (101)
3	3.100	1	413.9
6	6.060	1	257.4
10	10.040 (10.27)	2 (2)	174.5 (18.6)
16	30.016	2.5	115.7
30	—	3	67.3
60	—	4	38.6
100	—	5 (5)	25.92 (2.93)
150	—	10	19.3
300	—	20	12.44
400		30	10.71

Values in brackets indicate the corresponding value for alpha particle. The symbol '—' in the second column indicates that specific energies calculated at the centre of the cell nucleus coincide with the initial energy (energy losses before reaching the centre are negligible).

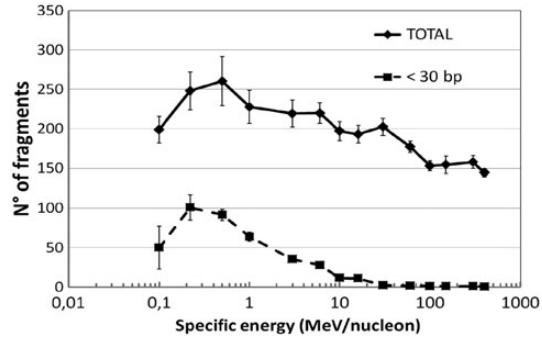

Figure 2. Number of fragments vs. specific energy for 2-Gy irradiations with carbon ions. Error bars are standard deviations ($\pm 1\sigma$). Lines are a guide for the eye.

CONCLUSIONS

Carbon-induced DNA damage is investigated with PARTRAC in a wide range of energy and LET, and results are given in terms of DSBs/CLs induction. The largest amount of DNA fragments in the range of <1 kbp (corresponding to a higher level of damage complexity, hence of biological effectiveness) is found for carbon-specific energies of <6 MeV u^{-1}. Carbon fragmentation in tissue is known to be a relevant process to be taken into account in carbon

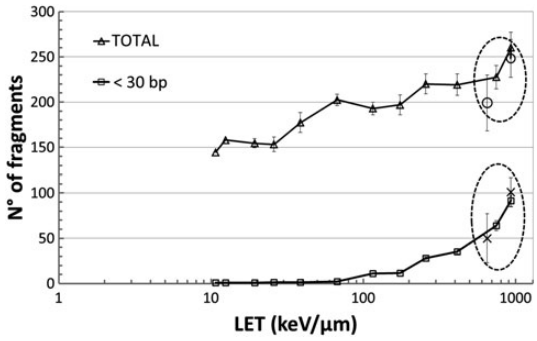

Figure 3. Number of fragments vs. LET for 2-Gy irradiations with carbon ions. Error bars are standard deviations ($\pm 1\sigma$), and lines are a guide for the eye. Circles in the curve relative to 'total' number of fragments and cross symbols 'X' relative to fragments of <30 bp, respectively, indicate the results in the narrow zone around the maximum LET, where the damage has been evaluated for equal LET values (put in evidence by a dashed circle) at the two opposite sides of the Bragg peak. See the text for more details.

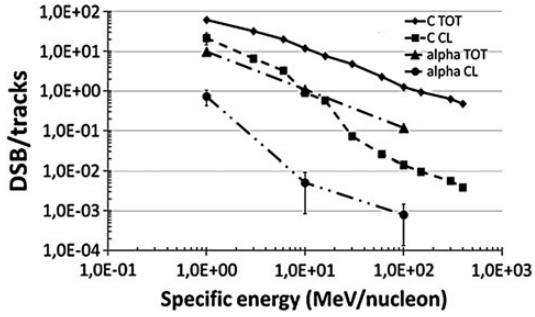

Figure 4. Comparison between DSBs or CLs per track vs. specific energy for C ions and alpha particles in the energy range of >1 MeV u^{-1}. Error bars are standard deviations ($\pm 1\sigma$, smaller than the symbols when not visible). Lines are drawn to guide the eye.

therapy, modifying radiation quality and therefore dose delivery along the track. In this work, the authors have performed preliminary PARTRAC calculations to investigate DNA-damage induction from carbon break-up in three alphas with the same specific energy, compared with carbon directly induced damage. For specific energies of >1 MeV u^{-1}, DSB or CL yields per track were calculated, and a factor 3 was applied to compare secondary alpha- and C-induced damage. The relative global effectiveness of the three alphas with respect to the primary carbon is found to be maximal for the minimal and maximal considered alpha energies: the authors may think of these two cases as fragmentation occurring at the end of the path of a slowed down carbon, or at the

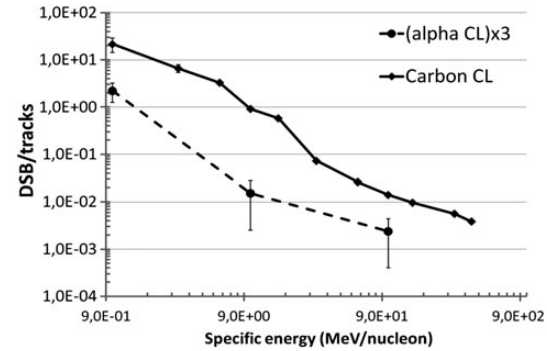

Figure 5. CLs/track vs. specific energy for C ions, compared with the same quantity for alphas, after the multiplication by a factor 3, in the energy range of >1 MeV u^{-1}. Error bars are standard deviations ($\pm 1\sigma$, smaller than the symbols when not visible). Lines are a guide for the eye.

beginning of the track for a high-energy ion. A further characterisation of secondary charged particle production due to carbon interactions is foreseen, through transport codes as PHITS[18] or MCNP6. Transport calculations of this kind can be further coupled to track structure models[19], thus extending in a systematic way the presented study of DNA damage from primary carbon and secondary products in a wider energy range and also to specific biological target geometries.

FUNDING

This work was partially supported by the European Commission (EC Contract FP7-249689 'DoReMi').

REFERENCES

1. Alloni, D. *et al. Charged particle effects: experimental and theoretical studies on the mechanisms underlying the induction of molecular and cellular damage and the modulation of intercellular signalling*. Nuovo Cimento **31**(C), 20–38 (2008).
2. Alloni, D., Campa, A., Friedland, W., Mariotti, L. and Ottolenghi, A. *Track structure, radiation quality and initial radiobiological events: considerations based on the PARTRAC code experience*. Int. J. Radiat. Biol. **88** (1–2), 77–86 (2012).
3. Goodhead, D. T. *Initial events in the cellular effects of ionising radiations: clustered damage in DNA*. Int. J. Radiat. Biol. **65**, 7–17 (1994).
4. Alloni, D., Campa, A., Facoetti, A., Friedland, W., Liotta, M., Mariotti, L., Paretzke, H. G. and Ottolenghi, A. *A Monte Carlo study of radiation quality dependence of DNA fragmentation spectra*. Radiat. Res. **173**(3), 263–271 (2010).
5. Alloni, D., Campa, A., Belli, M., Esposito, G., Mariotti, L., Liotta, M., Friedland, W., Paretzke, H. G. and Ottolenghi, A. *Monte Carlo evaluation of DNA*

fragmentation spectra induced by different radiation qualities. Radiat. Prot. Dos. **143**(2–4), 226–231 (2011).
6. Alloni, D., Campa, A., Friedland, W., Mariotti, L. and Ottolenghi, A. *Small DNA fragments induced by high-LET radiations: the Monte Carlo computation and its comparison with experimental data*. Radiat. Res. **179**(6), 690–697 (2013).
7. Mariotti, L., Facoetti, A., Bertolotti, A., Ranza, E., Alloni, D. and Ottolenghi, A. *Radiation induced perturbation of cell-to-cell signaling and communication*. Radiat. Prot. Dosim. **143**(2–4), 294–300 (2011).
8. Mariotti, L., Bertolotti, A., Ranza, E., Babini, G. and Ottolenghi, A. *Investigation of the mechanisms underpinning IL-6 cytokine release in bystander phenomena: the roles of radiation dose, radiation quality and specific ROS/RNS scavengers.* Int. J. Radiat. Biol. **88**(10), 751–762 (2012).
9. Nikjoo, H., Uehara, S., Emfietzoglou, D. and Cucinotta, F. A. *Track-structure codes in radiation research*. Radiat. Meas. **41**, 1052–1074 (2006).
10. Friedland, W., Jacob, P., Paretzke, H. G., Ottolenghi, A., Ballarini, F. and Liotta, M. *Simulation of light ion induced DNA damage patterns.* Radiat. Prot. Dosim. **122**, 116–120 (2006).
11. Schardt, D., Elsässer, T. and Schulz-Ertner, D. *Heavy-ion tumor therapy: physical and radiobiological benefits.* Rev. Mod. Phys. **82**, 383–425 (2010).
12. Hultqvist, M., Lazzeroni, M., Botvina, A., Gudowska, I., Sobolevsky, N. and Brahme, A. *Evaluation of nuclear reaction cross-sections and fragment yields in carbon beams using the SHIELD-HIT Monte Carlo cod. Comparison with experiments.* Phys. Med. Biol. **57**, 4369–4385 (2012).
13. Haettner, E., Iwase, H., Krämer, M., Kraft, G. and Schardt, D. *Experimental study of nuclear fragmentation of 200 and 400 MeV/u 12C ions in water for applications in particle therapy.* Phys. Med. Biol. **58**, 8265–8279 (2013).
14. Kraft, G., Krämer, M. and Scholz, M. *LET, track structure and models.* Radiat. Environ. Biophys. **31**, 161–180 (1992).
15. Schmitt, E., Friedland, W., Kundrat, P., Dingfelder, M. and Ottolenghi, A. *Track-structure modelling for low-energy light ions in PARTRAC*. Rad. Prot. Dosim., this issue (2015).
16. Alloni, D., Ballarini, F., Belli, M., Campa, A., Esposito, G., Friedland, W., Liotta, M., Ottolenghi, A. and Paretzke, H. G. *Modeling of DNA fragmentation induced in human fibroblasts by ^{56}Fe ions.* Adv. Space Res. **40**, 1401–1407 (2007).
17. Campa, A., Alloni, D., Antonelli, F., Ballarini, F., Belli, M., Dini, V., Esposito, G., Facoetti, A., Friedland, W. and Tabocchini, M. A. *DNA fragmentation induced in human fibroblasts by 56Fe ions: experimental data and Monte Carlo simulations.* Radiat. Res. **171**, 438–445 (2009).
18. Sato, T. *et al*. *Particle and Heavy Ion Transport code System PHITS, version 2.52*. J. Nucl. Sci. Technol. **50**(9), 913–923 (2013).
19. Baiocco, G., Alloni, D., Babini, G., Mariotti, L. and Ottolenghi, A. *Reaction mechanism interplay in determining the biological effectiveness of neutrons as a function of energy.* Rad. Prot. Dosim., this issue (2015).